DciA secures bidirectional replication initiation in Vibrio cholerae

Amelie Besombes, Yazid Adam, Christophe Possoz, Ivan Junier, François–xavier Barre, Jean-Luc Ferat

Nucleic Acids Research, 2024, **52**, 12324–12333
https://doi.org/10.1093/nar/gkae795
Advance access publication date: 18 September 2024
Genome integrity, repair and replication

DciA secures bidirectional replication initiation in *Vibrio cholerae*

Amelie Besombes[1,2,†], Yazid Adam[1,†], Christophe Possoz[2,†], Ivan Junier[3], Francois-Xavier Barre[2] and Jean-Luc Ferat[1,*]

[1]Institute Jacques Monod (UMR 7592) Paris-Cité University / CNRS, 15 rue Hélène Brion 75013 Paris, CEDEX 13, France
[2]Paris-Saclay University, CEA, CNRS, Institute for Integrative Biology of the Cell (I2BC), 1 avenue de la Terrasse 91198 Gif-sur-Yvette, France
[3]Univ. Grenoble Alpes, CNRS, UMR 5525, VetAgro Sup, Grenoble INP, TIMC, 5 Avenue du Grand Sablon 38700 La Tronche, France

[*]To whom correspondence should be addressed. Tel: +33 01 57 27 81 02; Email: jean-luc.ferat@ijm.fr
[†]The first three authors should be regarded as Joint First Authors.

Abstract

Replication is initiated bidirectionally in the three domains of life by the assembly of two replication forks at an origin of replication. This is made possible by the recruitment of two replicative helicases to a nucleoprotein platform built at the origin of replication with the initiator protein. The reason why replication is initiated bidirectionally has never been experimentally addressed due to the lack of a suitable biological system. Using genetic and genomic approaches, we show that upon depletion of DciA, replication is no longer initiated bidirectionally at the origin of replication of *Vibrio cholerae* chromosome 1. We show that following unidirectional replication on the left replichore, nascent DNA strands at *ori*1 anneal to each other to form a double-stranded DNA end. While this DNA end can be efficiently resected in *recB*$^+$ cells, only a few cells use it to trigger replication on the right replichore. In most DciA-depleted cells, chromosome 1 is degraded leading to cell death. Our results suggest that DciA is essential to ensuring bidirectional initiation of replication in bacteria, preventing a cascade of deleterious events following unidirectional replication initiation.

Graphical abstract

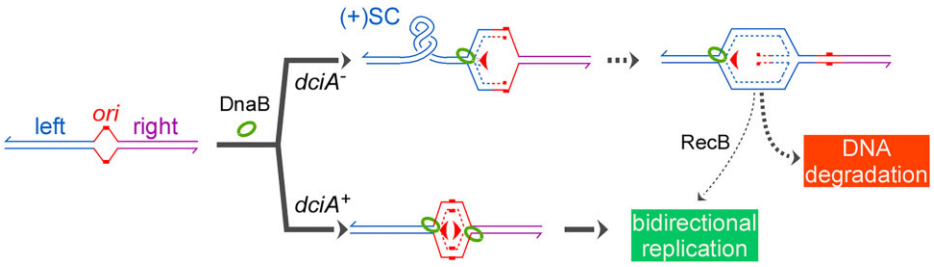

Introduction

Semi-conservative replication of genomic DNA requires DNA polymerase and replicative helicase activities. The latter is responsible for unwinding the double-stranded DNA (dsDNA) helix in front of the replication forks (RFs). In addition, replicative helicases ensure the processivity of DNA synthesis and maintain together the replication machinery of the leading and lagging strands so that both strands are simultaneously replicated. In the three domains of life, replication is initiated by the binding of an initiation protein (an initiator) to a specific origin of replication (a replicator), as initially postulated by Jacob and Brenner (1). Replication is initiated unidirectionally in some plasmids such as ColE1 (2) and mobile elements relying on rolling circle replication (3). Although replication is always initiated bidirectionally on chromosomes, a bidirectional replication can subsequently be converted to unidirectional replication either by a programmed inactivation or by accidental collapse of one RF (4). The rationale behind the ubiquity of bidirectional replication initiation (BRI) on chromosomes across the tree of life remains unclear.

Bidirectional replication initiation requires the recruitment of two replicative helicases to the origin of replication, whose loading and activation are ensured and supported by a wide variety of systems. In eukaryotes, the two replicative helicases are sequentially recruited and loaded onto the origin DNA by the Origin of Replication Complex during the G1 phase. The MCM (minichromosome maintenance) helicases are activated after the recruitment of Cdc45 and the hetero-tetrameric GINS complex upon entry into S phase. The CMG (Cdc45-MCM-GINS) complex forces the initial unwinding of DNA at

Received: April 4, 2024. **Revised:** August 27, 2024. **Editorial Decision:** August 28, 2024. **Accepted:** September 2, 2024

replication origins, leading to the synchronous positioning of the two helicases on ssDNA (5). In contrast, bacterial replicative helicases do not contribute to the initial unwinding of the origin since they are directly loaded onto ssDNA (6) and their efficient loading is facilitated by an accessory protein. These accessory proteins are diverse, mutually exclusive and essential (7–9). The first replicative helicase accessory proteins to be studied, DnaC in *Escherichia coli* and DnaI in *Bacillus subtilis*, were found to be indispensable to the loading of their cognate replicative helicase. However, they are sparsely represented. Indeed, the vast majority of bacteria possess another accessory protein, DciA, which is essential for life (8). Previous works demonstrated, however, that DciA is dispensable for the loading of the replicative helicase (10,11). This apparent conundrum raises the question of the essential function of DciA, and of bacterial helicase operators in general, during BRI. Here, we address this question by studying the function of DciA in *Vibrio cholerae*.

Materials and methods

Strains, media and growth conditions

The *V. cholerae* strains used in this study were derived from E7946 (*V. cholera* O1 serogroup, El Tor). YAV20: E7946 *loxP*[*dciA*] SpR *lacZ*::*cre* ZeoR (details of construction in Supplementary Figure S1), AB14 (*ori*1^{INV}): YAV20 inv[*glmU-mioC*] (details of construction in Supplementary Figure S5), AB23: YAV20 Δ*recB*::CmR. The Δ*recB* allele was created by replacement of the *recB* coding sequence by that of the chloramphenicol acetyl transferase (*cat*) gene in YAV20 with a plasmid *recB*UP [#1002-#1003]-*cat* [#1093-#577]-*recB*DW [#1004-#1005] (Supplementary Table S1). All constructions used to construct mutants were introduced by natural transformation, a process that transfers ssDNA in the cell, which induces homologous recombination (see below for method). Cells were grown in LB (Bactotryptone 10 g/l, Yeast extract 5 g/l, NaCl 5 g/l) or in minimal medium (KH_2PO_4 3 g/l, Na_2HPO_4 6 g/l, NaCl 0.5 g/l, NH_4Cl 1 g/l, thiamine 5 μg/ml, D-fructose 0.4%, $MgSO_4$ 1 mM, $CaCl_2$ 0.1 mM). Cultures were maintained in a steady state with a small-scale turbidostat that maintained cultures at a constant optical density (OD) by varying the dilution rate.

Natural transformation

Vibrio cholerae cells cultivated in LB medium at 37°C (until an OD_{600} of 0.1) were harvested and resuspended in an equivalent volume of natural transformation medium (KH_2PO_4 3 g/l, Na_2HPO_4 6 g/l, NaCl 0.5 g/l, NH_4Cl 1 g/l, $MgSO_4$ 32 mM, $CaCl_2$ 5 mM) and incubated for 20 h at 30°C with chitin chips to induce cell competency (12). Cells were washed and resuspended in an equal volume of fresh natural transformation medium. Between 200 and 500 ng of DNA (PCR amplification or plasmid) were added to 1 ml of this solution and further incubated for 24 h at 30°C. The cells were then plated on LB medium complemented with the appropriate antibiotic and incubated at 30°C. The plates were inspected daily for the appearance of transformants up to 7 days.

Flow cytometry

Cells to be analyzed were previously fixed by adding 5 volumes of 70% ethanol per volume of sample. Prior to analysis, cells are washed twice in filtered TE (Tris-HCl [pH 7.5] 10 mM, EDTA [pH 8] 1 mM), resuspended in TE supplemented with RNase A and propidium iodide (10 μg/ml, each) and incubated for 2 h at 37°C. Stained cells were analyzed on a PARTEC Particle Analyzing System, PASIII. A total of 100 000 cells were counted per run and data were analyzed with the Flow max software, version 2.52, and WinMDI 2.9.

Chr1 to Chr2 ratio quantification

Total genomic DNA of cells to be analyzed was extracted according to the cetyltrimethylammonium bromide (CTAB)/NaCl protocol (13) and quantitative PCR (qPCR) experiments were performed using the SsoAdvanced Universal SYBR Green Supermix (BioRad) on a CFX384 Touch Real Time PCR system (BioRad). Three couples of oligos were designed per chromosome; two at the origin of replication and one at the terminus (Supplementary Figure S2B). The relative amount of each chromosome in sorted cells was assessed as follow. A Cq value was attributed for the Chr1 and Chr2 of each population of cells by averaging the Cq of three independent amplifications at *gidA*, *mioC* and *ter*1 (Chr1) and at *parA2*, *rctB* and *ter*2 (Chr2). The ratio Chr2/Chr1 was then calculated for each population from the ΔCq value (Supplementary Table S2).

Marker frequency analysis

DNA to be analyzed was extracted with the Sigma GenElute® bacterial genomic DNA kit to generate a genomic library according to Illumina's protocol. The libraries and the sequencing were performed by the High-throughput Sequencing facility of the I2BC (https://www.i2bc.paris-saclay.fr/sequencing/ng-sequencing/, CNRS, Gif-sur-Yvette, France). Genomic DNA libraries were made with the 'Nextera DNA library preparation kit' (Illumina) following the manufacturer's recommendations. Reads were aligned against *V. cholerae* reference genome (using Burrows-Wheeler Aligner) and at each position were assigned the number of reads aligned (marker frequency, MF). An in-lab written MATLAB-based script (available on demand) was used to perform MF analysis. MF data (normalized by the total number of reads) are plotted in log2 against Chr1 and Chr2 sequences. Enrichment of unique mapping sequence reads were calculated over 1 kb-window and values deviating by >20% from the average were discarded from the analysis. For the most part, the sequencing bias corresponded to regions of low GC content that were associated with mobile elements, such as the Super Integron on Chr2, the Vibrio pathogenicity island (VPI-1 and VPI-2) and the Vibrio seventh pandemic islands (VSP-1 and VSP-2) on Chr1. Slopes were calculated to fit a simple linear regression model to the marker frequency (MF) data between coordinates 1/20th of Chr1 (∼150 kb) from *ori*1 and *ter*1, for right and left replichores (Supplementary Table S3). We designated arbitrarily the left replichore as the replichore on which *crtS* is located. Their projection was then calculated from the slopes to *ori*1. In ΔMF plots (Figure 3D), MF data of [*recB*$^-$*dciA*$^-$] cells cultivated for 12 h in arabinose were subtracted from MF data of the same cells cultivated for 20 h.

NSA-seq

Total genomic DNA (extracted according to the CTAB/NaCl protocol (13)) was resuspended in 50 μl Tris 5 mM (pH 8.5) and incubated overnight with RNase A (20 μg/ml) at 37°C. The resulting product was precipitated and resuspended in

50 µl Tris 5 mM solution. Total DNA was quantified using Qubit kit. Genomic DNA was then digested with *Mbo* I or *Sau3A* I (NEB) (*Mbo* I digestion: 12.5 units for 25 µg DNA, *Sau3A* I digestion: 2.5 units for 500 ng DNA. Digestions were performed as recommended by the supplier for 4 h at 37°C, precipitated and resuspended in H_2O. To create an overhanging TC 3′ end, the resuspended DNA was incubated with dATP and dGTP (0.1 mM each), DNA Polymerase I, Large (Klenow) and incubated for 30 min at 25°C and 20 min at 75°C.

DNA fragments of 0.1 to 1.5 kbp were purified by double side size selection (0.45–1.8×) according to the SPRIselect User Guide. Finally, the DNA fragments were eluted in Tris-HCl 5 mM (pH 8.5). DNA fragments were ligated to a linker (see oligo table) with T4 DNA ligase (1 h at 16°C). Linkers were added at a concentration of 15, 1.5 or 0.375 µM when 100–500, 10–100 or 1–10 ng DNA was available, respectively. Linker-ligated DNA fragments were purified twice from linker dimers with SPRIselect beads (0.9×). Purified DNA was amplified with G5 polymerase with 10 ng of DNA for 14 cycles. PCR products were purified twice with SPRIselect beads (0.9×). The quality of each library was checked with a bioanalyser kit. The sequencing was performed by the High-throughput Sequencing facility of the I2BC (https://www.i2bc.paris-saclay.fr/sequencing/ng-sequencing/, CNRS, Gif-sur-Yvette, France). Paired ends read were aligned to *V. cholerae* reference genome (using Burrows-Wheeler Aligner) and reads without 2 GATC or not mapping on an GATC site were discarded. Reads were summed over 100 kbp from *ori1* and *ori2* on the left and right replichore (*ori1* and *ori2* sequences were excluded) and normalized by the total number of reads. Data from the *Mbo* I digestion were normalized by those from the *Sau3A* I digestion. The mean and standard deviation around the mean were calculated from three independent experiments.

Results

Unidirectional initiation of replication in DciA-depleted cells

We worked in the *dciA*-containing gamma-proteobacterium *Vibrio cholerae*, which contains two chromosomes: Chr1, whose replicator (*ori*1) is typical of bacterial chromosomal origins and Chr2, whose replicator (*ori*2) is of plasmid origin. DciA being essential, we constructed a strain (*loxP*[*dciA*]), in which the *dciA* gene can be deleted, to investigate the requirement for DciA in the loading of the *V. cholerae* replicative helicase, DnaB, *in vivo*. In the *loxP*[*dciA*] strain, the *dciA* coding sequence is flanked with two *loxP* sites such that *dciA* can be excised upon induction of the Cre recombinase by arabinose. We followed the disappearance of DciA by western blot analysis after induction of the expression of the Cre recombinase and established that DciA becomes undetectable 4 h after induction (Supplementary Figure S1). Since the translocation of the replicative helicase in front of the replication machinery is indispensable for DNA synthesis during replication, we used replication as a reporter activity of the ability of the replicative helicase to be loaded on DNA. Cultures of the *loxP*[*dciA*] strain were brought to, and maintained under, steady state growth in minimal medium at 30°C prior to the addition of arabinose (see 'Materials and Methods' section) (14). Samples were taken 12, 16 and 20 h after addition (or not) of arabinose and directly analyzed by flow cytometry to follow over time the impact of the lack of DciA on cell growth. The growth rate of WT and DciA-depleted cells (henceforth designated as [*dciA*⁻] cells for simplicity) was observed to increase during the course of the experiment, resulting in a DNA content of one to two genomes per cell (Figure 1A and Supplementary Figure S2). Samples of cells taken 16 h after addition (or not) of arabinose were further incubated for 4 h with cephalexin in order to assess the amount of DNA synthesized in [*dciA*⁺] and [*dciA*⁻] cells (cephalexin

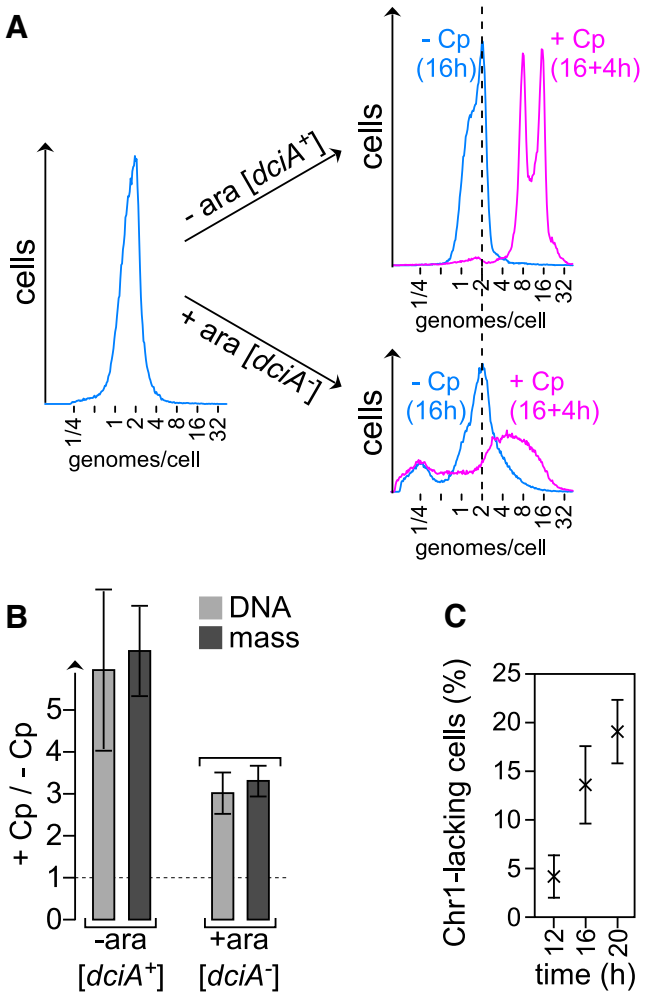

Figure 1. DciA-lacking cells perform complete rounds of replication. (**A**) DNA Cytograms of *loxP*[*dciA*] *V. cholerae* population maintained in steady state in minimal medium at 30°C for 16 h without (top) or with (bottom) arabinose (0.02% final concentration), and before (-Cp, cyan) or after (+Cp, magenta) incubation with cephalexin (Cp) for 4 h (1 µg/ml final concentration). Cephalexin blocks cell division without affecting the replication, enabling the measure of the amount of DNA synthesized during the incubation period. DNA content is indicated in logarithmic scale with 1 as the equivalent of one *V. cholerae* genome (4 Mbp) on the *x*-axis and the amount of cells in the *y*-axis. A dashed line indicates the position of cells containing two genomes. (**B**) The ratio '+ Cp / - Cp' was measured to assess cell growth (mass) and DNA synthesis (DNA) during a 4 h incubation with cephalexin (Cp). Prior to the addition of cephalexin, cells were grown for 16 h with (+ara [*dciA*⁻]) or without arabinose (-ara [*dciA*⁺]). The values presented correspond to the average and standard deviation of three independent experiments. (**C**) Accumulation of Chr1-lacking cells in population of [*dciA*⁻] cells, 12, 16 and 20 h after addition of arabinose. The values presented correspond to the average and standard deviation of three independent experiments.

is a cephalosporin, related to penicillins, which is used in our experiment at a concentration that blocks cell division without affecting replication or inducing detectable cell lysis). The mass of both types of cells treated with cephalexin increased as a consequence of the blockage of cell division, showing that [*dciA*$^-$] cells were still growing 20 h after addition of arabinose (Supplementary Figure S2A). The DNA content of [*dciA*$^+$] and [*dciA*$^-$] cells treated with cephalexin increased also, indicating that [*dciA*$^-$] cells can synthesize DNA 20 h after addition of arabinose, although [*dciA*$^-$] cells synthesized half the amount of that synthesized by [*dciA*$^+$] cells (Figure 1B). Overall, these data show that cell division and synthesis of DNA (in the absence of cephalexin) can be repeated several times in a row, despite the absence of DciA, suggesting that [*dciA*$^-$] cells can wholly replicate their genome (Supplementary Figure S2A). We also noticed the appearance of cells containing approximately one-fourth (∼1 Mbp) of the full *V. cholerae* genome in cultures of [*dciA*$^-$] cells (Figure 1A and Supplementary Figure S2A). These cells were sorted by FACS and a quantitative PCR analysis was performed using primer sets diagnostic for Chr1 and Chr2. This analysis revealed a ratio Chr2/Chr1 of 50, indicating that these cells do not contain Chr1 and solely Chr2 (Supplementary Figure S2B,C and Supplementary Table S2). It is noteworthy that the proportion of Chr1-lacking cells increases over time, raising from 4 ± 2% at 12 h to 15.7 ± 3.4% 20 h after addition of arabinose (Figure 1C).

To determine whether DNA synthesis observed in [*dciA*$^-$] cells by flow cytometry results from a genuine replication initiated at the origin of replication, we performed an MF analysis. We sequenced the whole genome in a population of asynchronously growing WT and [*dciA*$^-$] cells to measure the frequency of each position of the genome. In WT cells, the MF of sequences located at the origin of replication is at its highest, while that of sequences at the fork convergence sites (*fcs*), which are located at *ter*1 and *ter*2, is at its lowest, indicating that replication is initiated bidirectionally from a single origin of replication on each chromosome (Figure 2A and Supplementary Figure S3A) (15). The slope is about the same on each replichore of the two chromosomes, reflecting a homogeneous progression of the RFs, on each replichore. In contrast, the slopes of the left and right replichores of Chr1 are asymmetrical in [*dciA*$^-$] cells, revealing a replication defect (Figure 2B). We drew trend lines to symbolize the replication profile of the two cell types. The dark blue and purple trend lines cross each other at *ori*1 in [*dciA*$^+$] cells, indicating that replication was initiated bidirectionally at *ori*1 (Figure 2A). In contrast, the two trend lines cross the ordinate axis at two distinct points in [*dciA*$^-$] cells (Figure 2B), with a lower value on the right than on the left replichore. The difference between these two values, which we called $\delta_{ori1}{}^+$, may either reflect a deficit of replication of the right replichore or, alternatively, a delay in the initiation of the replication on the right replichore, after replication of part of the left replichore (Supplementary Figure S4). We simulated both scenarios and built theoretical MF profiles for each hypothesis (Supplementary Figure S4B,C). According to the 'delay in the initiation of the replication on the right replichore' hypothesis, the right replisome would be activated after 830 kbp (55%) of the left replichore of Chr1 had been replicated in [*dciA*$^-$] cells (Supplementary Figure S4B and Supplementary Data). Given the absence of RF trap in *V. cholerae* (15), a delay in the activation of the replisome on the right replichore would imply a displacement of the fork convergence site within the right replichore, at about 415 kbp of the *ter*1 site (Supplementary Data). Yet, the MF profile of [*dciA*$^-$] cells shows that replication of Chr1 is completed at *ter*1 (Figure 2B), which led us to rule out this hypothesis. In contrast, these results fit well with the 'deficit of replication on the right replichore' hypothesis, which proposes that at the onset of replication, a fraction of the cells initiate replication unidirectionally on the left replichore while in another fraction, replication of the left and right replichores is triggered at about the same time (Supplementary Figure S4B). Consistent with this scenario, the *fcs* remains at *ter*1 and the slope of the right replichore ($3.38 \times 10^{-7} \pm 0.37 \times 10^{-8}$ nucl.$^{-1}$) is much flatter than that of the left replichore ($-1.49 \times 10^{-7} \pm 0.16 \times 10^{-8}$ nucl.$^{-1}$) (Supplementary Figure S4C and Supplementary Data).

A careful analysis of the MF within the *ori*1 region shows an abrupt drop of MF within the first 130 kbp of the left replichore next to *ori*1, bringing the highest MF value around 130 kbp inside the left replichore and not at *ori*1 (Figure 2B, inset). To rule out the possibility that a dormant origin of replication be activated on the left replichore in [*dciA*$^-$] cells, we constructed a strain in which *ori*1 was inverted without changing the position of the potential dormant origin (Supplementary Figure S5). The MF profile of the *ori*1^{INV} strain is identical to that of the *ori*1$^+$ strain, indicating that the inversion of the origin of replication of Chr1 did not affect the replication program of the strain (Figure 2C). In a [*dciA*$^-$] background, the MF profile of the *ori*1^{INV} strain is, however, symmetrical to that obtained with the *ori*1$^+$ strain (Figure 2D). Both the highest MF value and an abrupt drop of MF are observed within the first 130 kbp adjacent to *ori*1, but on the right replichore (Figure 2D, inset). We conclude that there is no dormant origin of replication on either side of *ori*1 that is activated in [*dciA*$^-$] cells. Therefore, *ori*1 serves as a *bona fide* origin of replication of Chr1 in [*dciA*$^-$] cells, irrespective of the orientation of *ori*1. We calculated the δ value in *ori*1$^+$ and *ori*1^{INV} cells to estimate the percentage of cells in which the replication of only one replichore was initiated at *ori*1. Approximately 27 ± 2% of [*ori*1$^+$*dciA*$^-$] and 18 ± 1% of [*ori*1^{INV}*dciA*$^-$] of the cells analyzed by MF (Supplementary Table S3) did not replicate the right or the left replichore at *ori*1 at the onset of replication, respectively. Given that replication is initiated at *ori*1 in [*dciA*$^-$] cells, we conclude also that the abrupt drop of MF next to the origin on the left replichore (in *ori*1$^+$) or on the right replichore (in *ori*1^{INV}) must reflect the degradation of newly synthetized DNA (Figure 2A and B, right).

Surprisingly, the replication of Chr2 is initiated bidirectionally at *ori*2 in the absence of DciA and no DNA degradation is detected on either side of *ori*2 (Figure 2B and D). This indicates that the initiation of replication of Chr2 is unaffected by the lack of DciA and that the degradation of the newly replicated DNA next to *ori*1 is not an indirect consequence of the absence of DciA but correlated, instead, to the replication defect observed at *ori*1. Moreover, the amount of Chr2 in the population of [*dciA*$^-$] cells is larger than that of Chr1 (Figure 2B and D); it increases over the time of incubation with arabinose (Supplementary Figure S3B). In Vibrionales, the timing of replication initiation of Chr2 is strictly regulated and defined so that replication of Chr1 and Chr2 are completed synchronously (16). This is achieved by making replication initiation of Chr2 dependent on the replication of a site located on Chr1, *crtS* (17,18). This regulatory mechanism ensures that *Vibrio* cells contain as many Chr2 as Chr1. This led

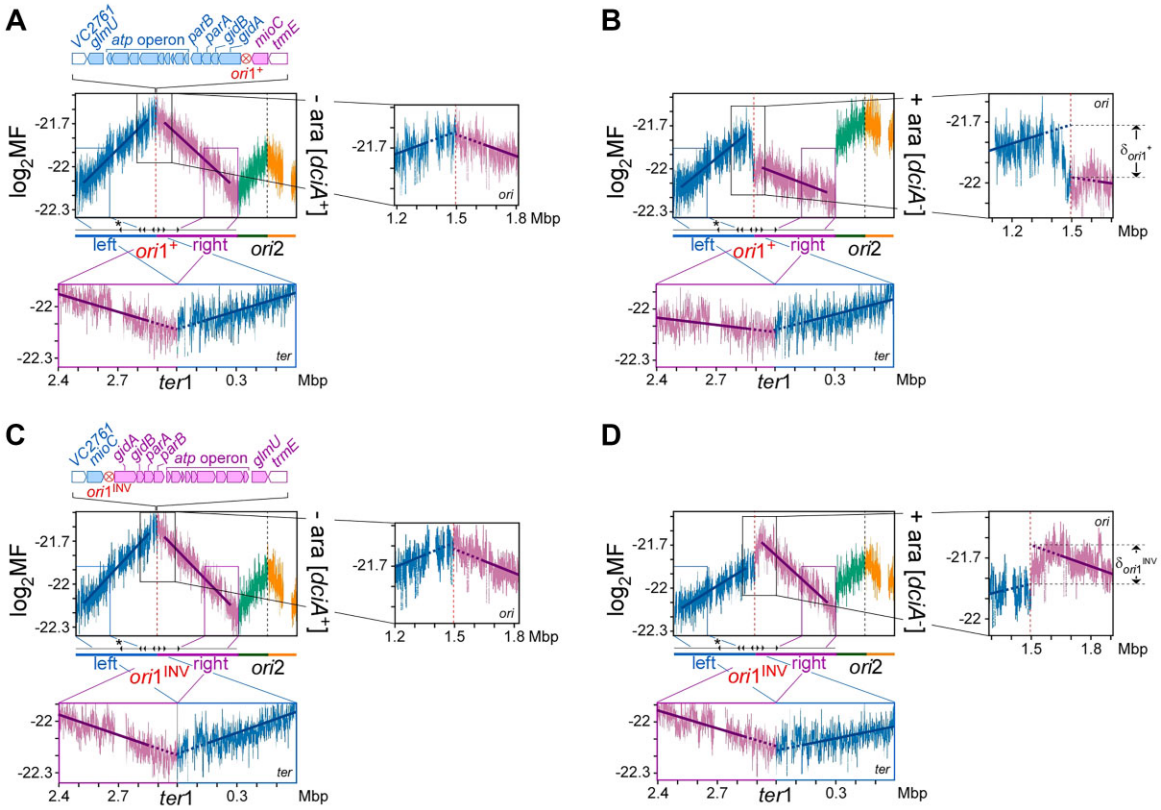

Figure 2. Replication is initiated unidirectionally at *ori*1 on Chr1 in [*dciA*$^-$] cells. (**A**) MF profile of a *ori*1$^+$ [*dciA*$^+$] (-ara) population maintained in continuous growth in minimal medium at 30°C for 12 h before DNA extraction and WGS library preparation. The reads were aligned against *V. cholerae* reference genome (using Burrows-Wheeler Aligner) to assign a number of reads per genome position (MF). The value for each position of the genome corresponds to the MF average of 1000 consecutive positions (1 kb) surrounding it. log2 of these values are used to account for the exponential growth of the cells. Finally, the value for each position is normalized by the total number of reads and plotted on Chr1 and Chr2 sequences (MATLAB). The left and right replichore of Chr1 and Chr2 are colored in blue, purple, green and orange, respectively. Details of the *ori*1 and *ter*1 regions are provided on the left and the bottom of the main MF. Trendlines were calculated for the left and right replichore assuming a constant progression of the RF (see materials and methods). Dashed lines indicate the projection of the trendlines on the ordinate axis at *ori*1 and *ter*1. Light red and black dashed lines report the position of *ori*1 and *ori*2. The position of ribosomal operons (arrow heads) and of *crtS* (*) are indicated below the MF (**B**) same as in (**A**), except that the cells are *ori*1$^+$ [*dciA*$^-$]. The projection of the trendlines for the left and right replichores cross the ordinate at *ori*1 at two different points, revealing a gap called $\delta_{ori1}{}^+$. (**C**) same as in (A) except that the orientation of *ori*1 was inverted *ori*1^{INV} [*dciA*$^+$]. (**D**) same as in (C) except that the cells are *ori*1^{INV} [*dciA*$^-$]. The projection of the trendlines for the left and right replichores also cross the ordinate at *ori*1 at two different points, revealing the gap $\delta_{ori1}{}^{INV}$. The genomic environment of *ori*1$^+$ and *ori*1^{INV} is provided.

us to rule out the possibility that supernumerary Chr2 be produced in [*dciA*$^-$] cells. We also excluded that a segregation defect in [*dciA*$^-$] cells resulted in the production of Chr1-lacking cells because the partition of Chr2 depends on that of Chr1 (19). Thus, we interpret the high Chr2/Chr1 ratio observed in MF analyses of [*dciA*$^-$] cells, together with the emergence of Chr1-lacking cells, as direct consequences of the degradation of Chr1.

RecB is essential to replicate DNA in [*dciA*$^-$] cells

As stated above, the MF profile of [*dciA*$^-$] cells suggests that if all cells initiate replication on the left replichore, only a fraction of these cells also trigger replication on the right replichore. This could simply be achieved by BRI. Alternatively, repair activities, such as those involved in the reactivation of RF, may be recruited at *ori*1 to trigger replication on the right replichore (20). To test this latter hypothesis, we constructed a Δ*recB loxP*[*dciA*] mutant strain, which is deficient in exonuclease V activity. The activity of exonuclease V, which consists in binding and resecting dsDNA ends, is neither required during replication initiation nor for the regular progression of RFs but becomes critical during replication reactivation (21). Δ*recB* cells grow poorly, likely due to the basal frequency at which RF are inactivated during unstressed replication. Indeed, exponentially growing Δ*recB* cells synthesize a very limited amount of DNA during a 4 h treatment with cephalexin compared to isogenic WT cells (compare Figure 3A and Figure 1A). The depletion of DciA in exponentially growing Δ*recB* ([*recB*$^-$ *dciA*$^-$]) cells worsens this phenotype (compare Figure 3B and Figure 3A) and the growth rate of [*recB*$^-$ *dciA*$^-$] cells is null after 12 h of incubation with arabinose (Supplementary Figure S6A), indicating that the association of *recB*$^-$ with *dciA*$^-$ is a synthetic lethal combination. Altogether, these data suggest that the activity of RecB becomes critical for replication in *dciA*$^-$ cells.

There are moderate differences between the MF profiles of *recB*$^-$ and *recB*$^+$ cells, whether in a [*dciA*$^+$] or in a [*dciA*$^-$] background (compare Figure 2A and Supplementary Figure S6B and compare t12 and t20 in Figure 3C and Supplementary Figure S3B). This was unexpected as replication is severely impacted by the lack of RecB (Figure 3A and B) but likely reflects the implication of RecB during RF reactivation; the linear decrease of MF from *ori*1 and *ori*2 to *ter*1 and *ter*2, respectively,

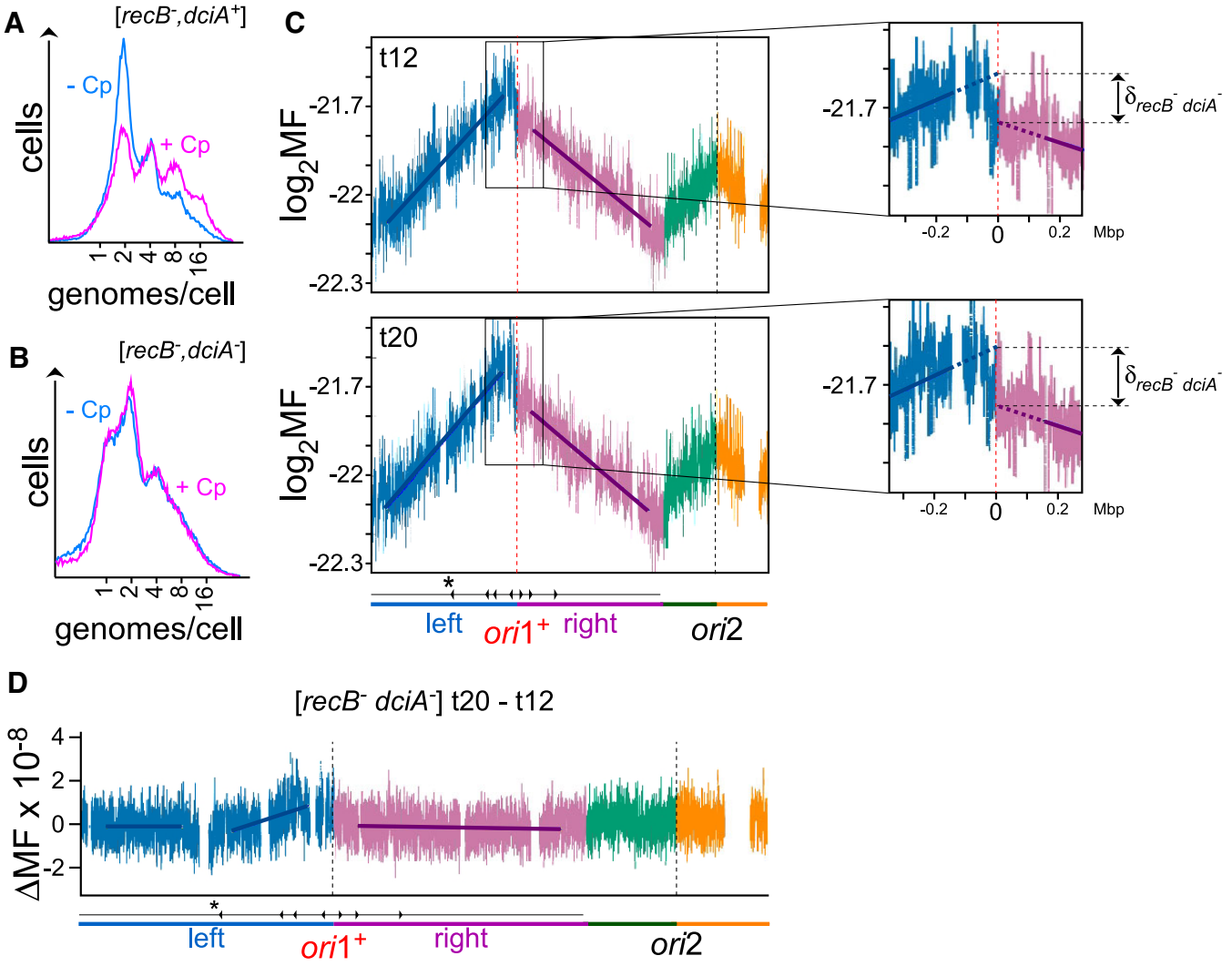

Figure 3. RecB is required for replication in [*dciA*⁻] cells. (**A**) DNA cytograms of [*recB*⁻ *dciA*⁺] cells cultivated for 12 h without arabinose, before (- Cp, blue profile), or after an incubation of 4 h with cephalexin (+ Cp, magenta profile). (**B**) Same as in (A) except that the cells were cultivated with arabinose [*recB*⁻*dciA*⁻]. (**C**) MF profiles of [*recB*⁻*dciA*⁻] cells 12 and 20 h after addition of arabinose (see legend of Figure 2 for description of symbols and features). $\delta_{recB\text{-}dciA\text{-}}$ was assessed as described in Figure 2. (**D**) MF of [*recB*⁻*dciA*⁻] cells cultivated for 12 h in arabinose was subtracted from that of the same cells cultivated for 20 h.

in *recB*⁻ cells accounts for the overlay of active replications, as well as replications initiated at *ori*1 and *ori*2, which stopped regularly afterwards and could not be reactivated.

Nevertheless, the MF profile of [*recB*⁻ *dciA*⁻] cells display a drop of MF on the left replichore next to *ori*1, although to a lesser extent than in [*recB*⁺ *dciA*⁻] cells (compare $\delta_{recB^-dciA^-}$ with δ_{ori1^+}). The drop of MF on the left side of *ori*1 covers a much narrower region (~30 kbp), indicating that this region is prone to degradation—likely due to the action of other exonucleases present in the cell, such as SbcCD (22)—but that RecB is the main nuclease involved in its resection in [*dciA*⁻] cells.

Replication is strictly initiated unidirectionally in [*dciA*⁻] cells

Our results, showing that RecB is required during replication in [*dciA*⁻] cells, suggest that a dsDNA end is generated at the onset of replication in [*dciA*⁻] cells. dsDNA ends are produced after a double strand break, when the DNA polymerase encounters a nick on the matrix strand during replication or after regression of newly synthesized strands into a chicken foot structure, such as during the reversion of RFs. In each case, except during a RF reactivation, the resection of the dsDNA end by exonuclease V, generating a 3′ single strand end, requires the following recruitment of RecA to promote DNA strand exchange (23). The reactivation of replication after RF reversal, on the other hand, may merely require the resection activity of the exonuclease V to reinstall an active RF (21). Hence, we investigated the implication of RecA during replication in [*dciA*⁻] cells. DNA cytograms of [*recA*⁻ *dciA*⁻] cells are almost identical to those obtained with [*recA*⁺ *dciA*⁻] cells, indicating that the lack of RecA does not impact [*dciA*⁻] cells growth (Supplementary Figure S6C). We conclude from these results that RecA is not required for replication in [*dciA*⁻] cells, which strongly supports the hypothesis according to which [*dciA*⁻] cells generate a chicken foot structure through regression of newly synthesized strands.

Given that RecB is not involved in replication initiation, we anticipated that replication is still initiated in [*recB*⁻ *dciA*⁻]

cells, with RFs progressing until their collapse. Hence, to detect traces of DNA synthesis or inversely a possible degradation of DNA in [*recB*$^-$ *dciA*$^-$] cells, we analyzed the subtraction of MF (ΔMF) obtained 12 and 20 h after depletion of DciA. This step eliminates the part of the MF profile corresponding to stalled or broken RF that were not reactivated. From 12 to 20 h, the growth rate is null, implying that the same cells are present from t12 to t20 in the turbidostat (Supplementary Figure S6A). Thus, values of ΔMF are indicative of DNA synthesis or DNA degradation. More precisely, and given that replication of Chr2 is unaffected by the lack of DciA, ΔMF values above those of Chr2 report DNA synthesis whereas those below those of Chr2 report DNA degradation. ΔMF analysis shows that DNA is exclusively produced on the left side of *ori*1—they are at their highest near *ori*1 and decrease regularly as one moves away from the origin (Figure 3D). We conclude from this analysis that replication is initiated in [*recB*$^-$ *dciA*$^-$] cells, exclusively on the left replichore. Consequently, the replication of the right replichore observed in [*dciA*$^-$] cells is replication initiation-independent and RecB-dependent. The regular decrease of the MF value from *ori*1 until mid left replichore (around *crtS*) likely accounts for the RF that collapsed and were not reactivated due to the absence of RecB.

Formation of a free dsDNA end at *ori*1 in [*dciA*$^-$] cells

A RecA-independent and RecB-dependent initiation of replication on the right replichore implies that a dsDNA end be formed, likely by regression of nascent DNA strands, upon unidirectional replication initiation. To test this hypothesis, we took advantage of the methylation status of GATC sites in *V. cholerae*. The methylation of GATC sites is a post-replicative process, i.e. the newly synthesized strand of DNA is unmethylated. Therefore, the newly replicated dsDNA behind the RF is hemimethylated (GATC$^{me/0}$) while that in front of the RF, not yet replicated, is fully methylated (GATC$^{me/me}$) (24). Given this starting situation, if two nascent and complementary strands of DNA anneal to each other, the dsDNA formed ought to be unmethylated (GATC$^{0/0}$) (Figure 4A).

We set up a new assay to identify Nascent Strands Annealing (which we called NSA-seq) to detect specifically unmethylated DNA. In brief, DNA from [*dciA*$^-$] and [*dciA*$^+$] cells was digested with restriction enzymes that are either sensitive (*Mbo* I) or not (*Sau3A* I) to the methylation status of the GATC sites; *Mbo* I cuts only GATC$^{0/0}$ sites while *Sau3A* I cuts all GATC sites (Figure 4A). The restriction fragments obtained after digestion with *Sau3A* I or *Mbo* I were sequenced and the reads containing a GATC site at each end of the sequenced fragments were retained ('Materials and Methods' section). The number of GATC site reads was summed over 100 kbp genomic segments starting from the left and right of *ori*1 and *ori*2 and divided by the total amount of reads (Supplementary Figure S7A,B). The [*dciA*$^-$]/[*dciA*$^+$] profile constructed with *Sau3A* I GATC fragments can be perfectly superimposed on that obtained with MF profiles of [*dciA*$^+$] and [*dciA*$^-$] cells (Supplementary Figure S7C), indicating that the amount of GATC fragments obtained by digestion of [*dciA*$^+$] and [*dciA*$^-$] total DNA is representative of an exponentially growing culture of these cells.

To investigate the overrepresentation of GATC$^{0/0}$ sites in the genome of [*dciA*$^-$] cells, we calculated the ratio *Mbo* I/*Sau3A* I to normalize the *Mbo* I values for the abundance of GATC sites (Figure 4B). The proportion of GATC$^{0/0}$ sites is relatively constant along Chr1 of [*dciA*$^+$] cells, showing no particular region where GATC$^{0/0}$ is overrepresented apart from the segment immediately on the right side of *ori*2 (Figure 4B). Yet, the emergence of this GATC$^{0/0}$ enriched region appears to be independent of DciA since it is present in the DNA of [*dciA*$^+$] and [*dciA*$^-$] cells. Consistent with the formation of a chicken foot intermediate on the left side of *ori*1 at the onset of replication in [*dciA*$^-$] cells, the analysis of the Chr1 of [*dciA*$^-$] cells further revealed a major GATC$^{0/0}$ enriched region immediately on the left side of *ori*1 (Figure 4B).

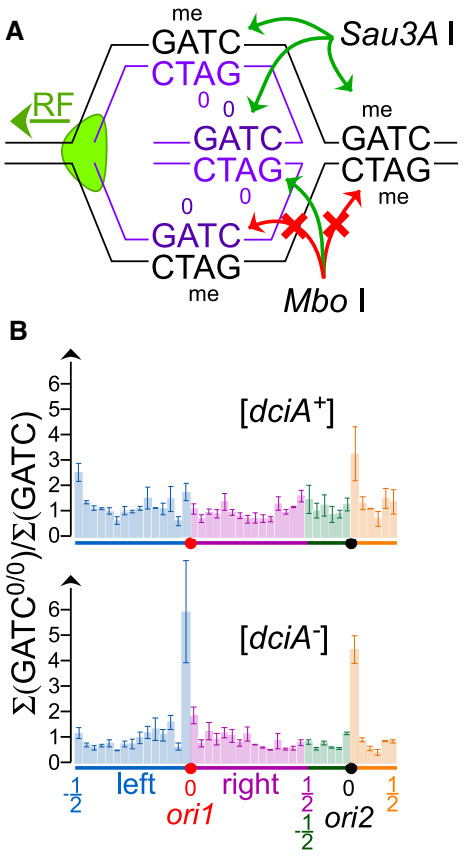

Figure 4. Lack of DciA induces annealing of nascent strands at *ori*1. (**A**) Sketch showing the three methylation status of DNA in *V. cholerae* with respect to replication. Before replication, DNA is fully methylated (GATC$^{me/me}$) while newly replicated DNA is hemimethylated (GATC$^{me/0}$). The regression of newly synthesized DNA strands (purple) generates an unmethylated dsDNA end (GATC$^{0/0}$), sensitive to *Mbo* I. GATC sites are sensitive to *Sau3A* I, irrespective of the methylation status of DNA. (**B**) DNA from [*dciA*$^+$] and [*dciA*$^-$] cells was digested with *Mbo* I and then sequenced. Unmethylated GATC fragments (GATC$^{0/0}$) of DNA were summed over 100 kbp from *ori*1 and *ori*2 on the right and left replichore. Each value was normalized by that obtained when DNA was digested with *Sau3A* I and plotted against the genome. NSA-seq was performed on DNA of [*dciA*$^+$] (top) and [*dciA*$^-$] cells (bottom). To prevent bias in the analysis, the sequences of *ori*1 and *ori*2 were excluded. Error bars correspond to the standard deviation around the mean value calculated from three independent experiments.

dsDNA end formation

As presented above, our results strongly suggest that a dsDNA end is formed at the onset of replication by regression of the nascent DNA strands next to *ori*1 on the left

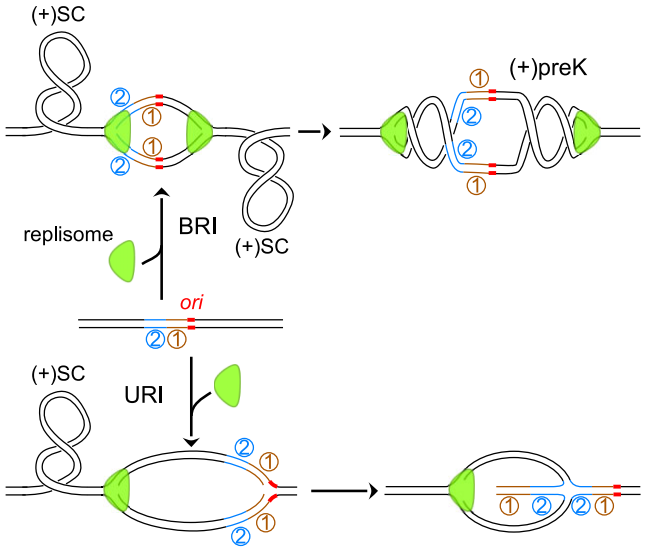

Figure 5. Outcomes of BRI and URI. Replication is initiated at *ori* (red rectangle) either bidirectionally (BRI) or unidirectionally (URI). (Top) BRI: DNA synthesis generates (+)SC in front of RFs, a fraction of which is converted into (+) precatenanes ((+)preK) in between RF. (Bottom) URI: DNA synthesis generates (+)SC in front of the single RF activated, a fraction of which may dissipate behind the RF, inducing the formation of a chicken foot intermediate.

replichore in [*dciA*$^-$] cells. Given that this process must be independent of RecA, we considered whether a mechanical strength—like that accumulating in positive supercoils ((+)SC) generated in front of a RF—could induce the regression of the nascent DNA strands and the formation of a dsDNA end located at the opposite end of the replication bubble when replication is initiated unidirectionally. During replication, (+)SC are mostly resolved by DNA gyrase (25). Some of them, however, may dissipate behind the RF by rotation of the RF around its own axis. This scenario was proposed to explain the formation of (+) precatenanes behind the RF (26). We investigated the possibility that the rotation of the RF may induce the annealing of the nascent DNA strands left free at the origin after unidirectional replication initiation by calculating and comparing the energetic cost of the formation of a dsDNA end versus that of (+) precatenanes (Figure 5). It is noteworthy that the annealing of nascent DNA strands following URI is distinct from the reversion of a RF because the latter occurs as a consequence of the inactivation of a RF, whereas the former occurs because an active RF replicates DNA (21). We therefore calculated the relative proportion of nascent DNA strands versus (+) precatenanes as a function of the number of RF rotations (Supplementary Data) (27,28). To this end, for a given number of rotations we estimated the energy associated with the formation of either (+) precatenanes, annealing of nascent DNA strands, or a combination of the two. The free energy cost of (+) precatenanes was estimated using the polymer theory of braided DNA molecules (29), while that of annealing of nascent DNA strands was set as the free energy cost of a Holliday junction (Figure 5). Strikingly, calculations show that any rotation of the RF preferentially leads to the annealing of nascent DNA strands (Supplementary Data) (27,28), i.e. the number of (+)SC converted in RF rotations should equal the number of turns of helix created at the other end of the replication bubble by annealing of nascent DNA strands (Figure 5 and Supplementary Figure S8). In other words, the progression of a RF activated during unidirectional replication initiation on the left replichore is predicted to generate a dsDNA end that extends with the progression of the RF.

Discussion

By analogy with DnaC, DciA was initially proposed to act as a replicative helicase loader (8). In the present study, we show, however, that [*dciA*$^-$] *V. cholerae* cells can initiate replication at *ori*1 and *ori*2 and complete several rounds of replication/division in a row, implying that DciA can no longer be considered as a loader or an activator of replicative helicases. Yet, and while [*dciA*$^-$] cells can replicate their genome, replication initiation of Chr1 is dysfunctional.

We carried out a series of experiments to gain insight into the initiation of replication in [*dciA*$^-$] cells and established that [*dciA*$^-$] cells initiate replication unidirectionally at *ori*1, on the left replichore. Replication of the right replichore is subsequently initiated in only a fraction of the cells (Figures 2 and 3). We further showed that this depends on RecB, which is part of the exonuclease V complex that recognizes and resects specifically dsDNA ends in bacteria (21). Importantly, we established that replication in [*dciA*$^-$] cells is not dependent on RecA, which excludes the possibility that double strand breaks be generated in [*dciA*$^-$] cells at the onset of replication. Chicken foot intermediates produced after RF collapse, on the other hand, solely depend on RecB to generate a forked structure on which the RF can be directly reactivated (i.e. without RecA).

We propose that following unidirectional replication initiation at *ori*1, a chicken foot DNA intermediate is produced by regression of the nascent DNA strands at *ori*1, which, after resection by RecB, serves as a forked structure to activate a RF that replicates the right replichore. The enrichment of unmethylated DNA on the left side of *ori*1 in [*dciA*$^-$] cells, reporting the regression of nascent DNA strands, strongly supports this model. Hence, a replication bubble would be produced at the onset of replication in [*dciA*$^-$] cells, which contains at one end a single active RF and at the other end, a dsDNA end resulting from the regression of the nascent DNA strands (Figure 5). How could such a dsDNA end be produced? The fact that replication of the right replichore is independent on RecA in [*dciA*$^-$] mutant cells led us to exclude, for example, that long stretches of ssDNA be produced upon replication initiation, and with it the possibility that a gap be created between the priming on the leading and lagging strand. At this moment, it is tempting to consider that the initial strength leading to the formation of the dsDNA end be induced by dissipation behind the RF of the (+)SC that are produced in front of the RF (Figure 5). Our calculation show, indeed, that in a replication bubble containing a single RF, the dissipation of (+)SC through the active RF within the replication bubble strongly favors the formation of a dsDNA end over that of a precatenane.

Thus far, our results imply that DciA ensures BRI of the bacterial chromosome in *V. cholerae*. The conservation of DciA and that of the mechanism of replication initiation in the bacterial domain (8) suggests that it probably plays the same function in other bacteria. In [*dciA*$^-$] cells, replication is strictly initiated unidirectionally on the left replichore of Chr1, suggesting that DciA serves to recruit a replicative helicase for the replication of the right replichore, and DnaA bringing the other helicase hexamer for the replication of the left replichore

(30). The structural homology between DciA and the domain I of DnaA (10), which interacts with the bacterial replicative helicase, DnaB (31), supports this hypothesis and suggests a mechanism through which DciA may connect the two hexamers of DnaB, which would be recruited as a whole by DnaA at *ori*1. According to this model, the joint action of DciA and DnaA synchronizes the recruitment of the two replicative helicases at the origin of replication to promote BRI. This model is particularly attractive as the crosstalk between the initiator (DnaA) and the helicase operator (DnaC) has also been proposed to ensure BRI in *E. coli* (32).

According to our MF analyses, only 30% of [*dciA*$^-$] cells fail to initiate replication of the right replichore, while the remaining 70% of [*dciA*$^-$] cells eventually establish a synchronous replication of the two replichores, i.e. in appearance, a majority of [*dciA*$^-$] cells behave like WT cells, by installing a bidirectional replication at origin of replication of the bacterial chromosome that ends at the terminus of the same chromosome (Figure 2). Given such numbers, why is *dciA* an essential gene? We identified an additional feature associated with the lack of DciA indicating that these cells represent only a fraction of the population.

[*dciA*$^-$] cells feature an aberrantly high Chr2/Chr1 ratio, which increases as a function of time, and the production of Chr1-lacking cells. As explained above, the replication of Chr2 is coordinated with that of Chr1 in *V. cholerae* through the duplication of the *crtS* site on Chr1, implying that there can never be more Chr2s than Chr1s. Therefore, an excess of Chr2 reveals that Chr1 was replicated and then markedly degraded in [*dciA*$^-$] cells, resulting in Chr1-lacking cells. The higher Chr2/Chr1 ratio in *ori*1$^+$ than in *ori*1^{INV} cells strongly supports this conclusion. In *ori*1$^+$ cells, the RF has to replicate around half the left replichore to reach *crtS*, whereas in *ori*1^{INV} cells, the RF has to completely replicate the right replichore, pass *ter*1 and replicate against the orientation of the genes around half of the left replichore. Because of the multiple transcription/replication conflicts that will encounter the RF of *ori*1^{INV} cells during the replication of the left replichore, it is likely that less RF will reach *crtS* in *ori*1^{INV} than in *ori*1$^+$ cells. Consequently, less Chr2 will be duplicated in *ori*1^{INV} than in *ori*1$^+$ cells, resulting in a lower Chr2/Chr1 ratio in *ori*1^{INV} than in *ori*1$^+$ cells.

At this stage, the cause for Chr1 degradation remains unknown, despite it being an important question, that we are currently addressing. We also do not know why the *ori*2 region is enriched in unmethylated DNA, irrespective of the absence or the presence of DciA. Is this likely to be a feature that will help us better understand the replication of Chr2? Indeed, the recruitment of the replicative helicase at *ori*2 during replication initiation remains largely elusive. Based on the observations that DnaA is essential for replication initiation at *ori*2 but unnecessary for the formation of an open complex, DnaA was shown to contribute to the recruitment of the replicative helicase for the replication of Chr2 (33). *ori*2 contains, however, only one DnaA box, suggesting that another factor—distinct from DciA—ensures the coordinated recruitment of the second replicative helicase during replication initiation. It will be interesting to understand how BRI is being implemented at *ori*2. It currently appears to be through a sequential but coordinated activation of the two replicative helicases.

An intriguing and still open question is the priming of the leading strand during replication initiation. It was proposed that upon loading of the two replicative helicases at *oriC* in *E. coli*, their translocation on their respective lagging strand also promotes the priming of the leading strand of the opposite replichore, suggesting that BRI was necessary to synthesize both leading strands during replication (34). On the other hand, Yeeles and Marians observed in an *in vitro* system that DNA synthesis on the leading strand can be re-primed during DNA synthesis, suggesting that a single replicative helicase can promote primer synthesis on both the leading and the lagging strands (35). Yet, in this experiment, replication was re-primed and not primed. It would be interesting to further address the question of the priming of DNA synthesis when replication is initiated unidirectionally.

Data availability

The illumina data are accessible at https://www.ncbi.nlm.nih.gov/sra/PRJNA1095475.

Supplementary data

Supplementary Data are available at NAR Online.

Acknowledgments

We warmly thank Rita Cha, Marie-Noelle Prioleau, Julien Bischerour and Pierre Brezellec for fruitful discussions and comments on the present manuscript and Lila J. Ferat for editing the English.

Author contributions: Conceptualization: C.P., J.-L.F. Methodology: A.B., Y.A., C.P., F.-X.B., J.-L.F. Investigation: A.B., Y.A., C.P., F.-X.B., J.-L.F. Modelization: I.J. Funding acquisition: F.-X.B., J.-L.F. Project administration: J.-L.F. Supervision: J.-L.F. Writing—original draft: J.-L.F. Writing—review and editing: A.B., Y.A., C.P., I.J., F.-X.B., J.-L.F.

Funding

Agence Nationale de la Recherche [23-CE12-0005-01 to J.-L.F.; 2016-CE12-0030-0 to F.-X.B.]; Fondation pour la Recherche Médicale [EQU202003010328 to F.-X.B.]. Funding for open access charge: Agence Nationale de la Recherche [23-CE12-0005-01; 2016-CE12-0030-0]; Fondation pour la Recherche Médicale [EQU202003010328].

Conflict of interest statement

The authors declare that they have no competing interests. Data and materials availability: All data are available in the main text or the Supplementary Data.

References

1. Jacob,F. and Brenner,S. (1963) [On the regulation of DNA synthesis in bacteria: the hypothesis of the replicon]. *C. R. Hebd. Seances Acad. Sci.*, **256**, 298–300.
2. Dasgupta,S., Masukata,H. and Tomizawa,J. (1987) Multiple mechanisms for initiation of ColE1 DNA replication: DNA synthesis in the presence and absence of ribonuclease H. *Cell*, **51**, 1113–1122.
3. Khan,S.A. (2000) Plasmid rolling-circle replication: recent developments. *Mol. Microbiol.*, **37**, 477–484.
4. Xie,B.B., Rong,J.C., Tang,B.L., Wang,S., Liu,G., Qin,Q.L., Zhang,W., She,Q., Chen,Y., Li,F., *et al.* (2021) Evolutionary

trajectory of the replication mode of bacterial replicons. *mBio*, **12**, e02745-20.
5. Lewis,J.S., Gross,M.H., Sousa,J., Henrikus,S.S., Greiwe,J.F., Nans,A., Diffley,J.F.X. and Costa,A. (2022) Mechanism of replication origin melting nucleated by CMG helicase assembly. *Nature*, **606**, 1007–1014.
6. Fernandez,A.J. and Berger,J.M. (2021) Mechanisms of hexameric helicases. *Crit. Rev. Biochem. Mol. Biol.*, **56**, 621–639.
7. Davey,M.J. and O'Donnell,M. (2003) Replicative helicase loaders: ring breakers and ring makers. *Curr. Biol.*, **15**, R594–R6.
8. Brézellec,P., Vallet-Gely,I., Possoz,C., Quevillon-Cheruel,S. and Ferat,J.-L. (2016) DciA is an ancestral replicative helicase operator essential for bacterial replication initiation. *Nat. Commun.*, **7**, 13271.
9. Brézellec,P., Petit,M.A., Pasek,S., Vallet-Gely,I., Possoz,C. and Ferat,J.-L. (2017) Domestication of lambda phage genes into a putative third type of replicative helicase matchmaker. *Genome Biol. Evol.*, **9**, 1561–1566.
10. Marsin,S., Adam,Y., Cargemel,C., Andreani,J., Baconnais,S., Legrand,P., Li de la Sierra-Gallay,I., Humbert,A., Aumont-Nicaise,M., Velours,C., *et al.* (2021) Study of the DnaB:DciA interplay reveals insights into the primary mode of loading of the bacterial replicative helicase. *Nucleic Acids Res.*, **49**, 6569–6586.
11. Ozaki,S., Wang,D., Wakasugi,Y., Itani,N. and Katayama,T. (2022) The Caulobacter crescentus DciA promotes chromosome replication through topological loading of the DnaB replicative helicase at replication forks. *Nucleic Acids Res.*, **50**, 12896–12912.
12. Meibom,K.L., Blokesch,M., Dolganov,N.A., Wu,C.Y. and Schoolnik,G.K. (2005) Chitin induces natural competence in *Vibrio cholerae*. *Science*, **310**, 1824–1827
13. Ausubel,F.M., Brent,R., Kingston,R.E., Moore,D.D., Seidman,J.G., Smith,J.A. and Struhl,K. (1987) In: *Current Protocols in Molecular Biology*. Wiley-Interscience, Hoboken, New Jersey, USA.
14. Hoffmann,S.A., Wohltat,C., Müller,K.M. and Arndt,K.M. (2017) A user-friendly, low-cost turbidostat with versatile growth rate estimation based on an extended Kalman filter. *PLoS One*, **12**, e0181923.
15. Galli,E., Ferat,J.-L., Desfontaines,J.M., Val,M.E., Skovgaard,O., Barre,F.X. and Possoz,C. (2019) Replication termination without a replication fork trap. *Sci. Rep.*, **9**, 8315.
16. Kemter,F.S., Messerschmidt,S.J., Schallopp,N., Sobetzko,P., Lang,E., Bunk,B., Spröer,C., Teschler,J.K., Yildiz,F.H., Overmann,J., *et al.* (2018) Synchronous termination of replication of the two chromosomes is an evolutionary selected feature in Vibrionaceae. *PLoS Genet.*, **14**, e1007251.
17. Val,M.E., Marbouty,M., de Lemos Martins,F., Kennedy,S.P., Kemble,H., Bland,M.J., Possoz,C., Koszul,R., Skovgaard,O. and Mazel,D. (2016) A checkpoint control orchestrates the replication of the two chromosomes of *Vibrio cholerae*. *Sci. Adv.*, **2**, e1501914.
18. Ramachandran,R., Ciaccia,P.N., Filsuf,T.A., Jha,J.K. and Chattoraj,D.K. (2018) Chromosome 1 licenses chromosome 2 replication in *Vibrio cholerae* by doubling the crtS gene dosage. *PLoS Genet.*, **14**, e1007426.
19. Chodha,S.S., Brooks,A.C., Davis,P.J., Ramachandran,R., Chattoraj,D.K. and Hwang,L.C. (2023) Kinetic principles of ParA2-ATP cycling guide dynamic subcellular localizations in *Vibrio cholerae*. *Nucleic Acids Res.*, **51**, 5603–5620.
20. Heller,R.C. and Marians,K.J. (2007) Non-replicative helicases at the replication fork. *DNA Repair (Amst.)*, **6**, 945–952.
21. Michel,B., Sinha,A.K. and Leach,D.R.F. (2018) Replication fork breakage and restart in *Escherichia coli*. *Microbiol. Mol. Biol. Rev.*, **82**, e00013-18.
22. Dimude,J.U., Midgley-Smith,S.L. and Rudolph,C.J. (2018) Replication-transcription conflicts trigger extensive DNA degradation in *Escherichia coli* cells lacking RecBCD. *DNA Repair (Amst.)*, **70**, 37–48
23. Bianco,P.R., Tracy,R.B. and Kowalczykowski,S.C. (1998) DNA strand exchange proteins: a biochemical and physical comparison. *Front. Biosci.*, **3**, D570–D603.
24. Campbell,J.L. and Kleckner,N. (1988) The rate of Dam-mediated DNA adenine methylation in *Escherichia coli*. *Gene*, **74**, 189–190.
25. Wang,J.C. (1991) DNA topoisomerases: why so many? *J. Biol. Chem.*, **266**, 6659–6662.
26. Peter,B.J., Ullsperger,C., Hiasa,H., Marians,K.J. and Cozzarelli,N.R. (1998) The structure of supercoiled intermediates in DNA replication. *Cell*, **94**, 819–827.
27. El Sayyed,H., Le Chat,L., Lebailly,E., Vickridge,E., Pages,C., Cornet,F., Cosentino Lagomarsino,M. and Esp´eli,O. (2016) Mapping topoisomerase IV binding and activity sites on the *E. coli* genome. *PLos Genet.*, **12**, e1006025.
28. Junier,I., Ghobadpour,E., Espeli,O. and Everaers,R. (2023) DNA supercoiling in bacteria: state of play and challenges from a viewpoint of physics based modeling. *Front. Microbiol.*, **14**, 1192831.
29. Marko,J.F. (1997) Supercoiled and braided DNA under tension. *Phys. Rev. E*, **55**, 1758.
30. Sutton,M.D., Carr,K.M., Vicente,M. and Kaguni,J.M. (1998) *Escherichia coli* DnaA protein. The N-terminal domain and loading of DnaB helicase at the *E. coli* chromosomal origin. *J. Biol. Chem.*, **273**, 34255–34262.
31. Seitz,H., Weigel,C. and Messer,W. (2000) The interaction domains of the DnaA and DnaB replication proteins of *Escherichia coli*. *Mol. Microbiol.*, **37**, 1270–1279.
32. Mott,M.L., Erzberger,J.P., Coons,M.M. and Berger,J.M. (2008) Structural synergy and molecular crosstalk between bacterial helicase loaders and replication initiators. *Cell*, **135**, 623–634.
33. Gerding,M.A., Chao,M.C., Davis,B.M. and Waldor,M.K. (2015) Molecular dissection of the essential features of the origin of replication of the second *Vibrio cholerae* chromosome. *mBio*, **6**, e00973.
34. Fang,L., Davey,M.J. and O'Donnell,M. (1999) Replisome assembly at oriC, the replication origin of *E. coli*, reveals an explanation for initiation sites outside an origin. *Mol. Cell*, **4**, 541–553.
35. Yeeles,J.T. and Marians,K.J. (2011) The *Escherichia coli* replisome is inherently DNA damage tolerant. *Science*, **334**, 235–238.

Received: April 4, 2024. **Revised:** August 27, 2024. **Editorial Decision:** August 28, 2024. **Accepted:** September 2, 2024